




Article

Surface Functionalization of Polyethylene by Silicon Nitride Laser Cladding

Matteo Zanocco^{1,2}, Elia Marin^{1,3} , Francesco Boschetto^{1,2}, Tetsuya Adachi³ , Toshiro Yamamoto³, Narisato Kanamura³, Wenliang Zhu¹, Bryan J. McEntire⁴ , B. Sonny Bal⁴, Ryutarō Ashida⁵, Osam Mazda² and Giuseppe Pezzotti^{1,2,6,7,*}

¹ Ceramic Physics Laboratory, Kyoto Institute of Technology, Sakyo-ku, Matsugasaki, Kyoto 606-8585, Japan; matteo.zanocco@gmail.com (M.Z.); elia-marin@kit.ac.jp (E.M.); boschetto.cesc@gmail.com (F.B.); wlzhu@kit.ac.jp (W.Z.)

² Department of Immunology, Graduate School of Medical Science, Kyoto Prefectural University of Medicine, Kamigyo-ku, 465 Kajii-cho, Kawaramachi dori, Kyoto 602-0841, Japan; mazda@koto.kpu-m.ac.jp

³ Department of Dental Medicine, Graduate School of Medical Science, Kyoto Prefectural University of Medicine, Kamigyo-ku, Kyoto 602-8566, Japan; t-adachi@koto.kpu-m.ac.jp (T.A.); yamamoto@koto.kpu-m.ac.jp (T.Y.); kanamura@koto.kpu-m.ac.jp (N.K.)

⁴ SINTX Technologies Corporation, 1885 West 2100 South, Salt Lake City, UT 84119, USA; BMcEntire@sintx.com (B.J.M.); SBal@sintx.com (B.S.B.)

⁵ Shinsei, Co., Shijohei Kawanishi Rikobo, Kyoto 610-0101, Japan; r.ashida@mold-shinsei.co.jp

⁶ Department of Orthopedic Surgery, Tokyo Medical University, 6-7-1 Nishi-Shinjuku, Shinjuku-ku, Tokyo 160-0023, Japan

⁷ The Center for Advanced Medical Engineering and Informatics, Osaka University, Yamadaoka, Suita, Osaka 565-0871, Japan

* Correspondence: pezzotti@kit.ac.jp

Received: 18 March 2020; Accepted: 1 April 2020; Published: 10 April 2020



Abstract: Functional coatings are commonly applied to biomaterials in order to improve their properties. In this work, polyethylene was coated with a silicon nitride (Si_3N_4) powder using a pulsed laser source in a nitrogen gas atmosphere. Several analytical techniques were used to characterize the functionalized surface of the polymer, including Raman spectroscopy, laser microscopy, scanning electron microscopy (SEM), and energy dispersive X-ray spectroscopy (EDS). Antibacterial properties were tested in vitro against *Staphylococcus epidermidis*. The Si_3N_4 coating sensibly reduced the amount of living bacteria when compared to the uncoated polymer. Osteoconductivity was also tested in vitro using SaOS-2 osteosarcoma cells. The presence of Si_3N_4 coating resulted in an increased amount of hydroxyapatite. Coating of polyethylene with silicon nitride may lead to improved performance of indwelling orthopaedic or less invasive medical devices.

Keywords: laser cladding; polyethylene; silicon nitride; antibacterial; osteointegration

1. Introduction

Over the last three decades, polymeric materials have been extensively developed and used for a broad range of biomedical applications, from packaging and single-use invasive devices (e.g., catheters) to implantable prostheses (e.g., acetabular liners). However, only a limited number of these materials are considered to be biocompatible [1]. These include: polyethylene (PE), polypropylene (PP), polyurethane (PU), polytetrafluoroethylene (PTFE), poly(vinyl chloride) (PVC), polyamides (PA), polymethylmethacrylate (PMMA), polyacetal (PA), polycarbonate (PC), poly(-ethylene terephthalate) (PET), polyetheretherketone (PEEK), and polysulfone (PSU). Their biocompatibility is believed to be solely due to their bioinert nature. The most used materials belong to a family of low-cost technical

polymers, such as PE, PVC, PP, and polystyrene, while the remaining plastics comprise only a minor fraction of the medical market.

Technical polymers are selected and modified depending on their specific applications. For example, packaging materials are often coated with a barrier layer to protect them against damage by humidity and oxygen. Energetic photon [2,3], ion [4], and electron beam [5,6] processes are used to modify polymeric surfaces in different ways. Polymers can also be coated or combined with a second phase during synthesis to form polymer-matrix composites. In orthopaedics, PE [7] has been prepared as a composite using different dispersoids such as carbon black [8,9], ceramics (TiO_2 [10], Al_2O_3 [11], CaCO_3 [12], hydroxyapatite [13]), and metallic fibres [14].

Silicon nitride (Si_3N_4) is a structural non-oxide ceramic and a candidate for a number of orthopedic applications because of its high strength and toughness [15]. However, unlike polymers, it is not bioinert, but bioactive. Its unique surface chemistry provides it with antibacterial [16] and osteoconductive [17] characteristics. Silicon nitride is currently cleared for use as an intervertebral spacer in spinal fusion surgery [18].

In this paper, we attempted to functionalize the surface of bulk PE by coating it with activated Si_3N_4 powder. It was hypothesized that the Si_3N_4 coating would protect the polymer from oxidation while conferring both antibacterial and osteogenic properties. If true, this approach might be useful in improving the lifetime of PE while concurrently reducing the risk of infection and promoting osteointegration.

2. Materials and Methods

2.1. Samples Production

Low-density polyethylene pellets (Sigma-Aldrich, Darmstadt, Germany) were used to prepare substrates by melting at $125\text{ }^\circ\text{C}$ under a low vacuum (10 Pa), in order to remove residual bubbles. A rectangular silicone rubber molding ($80 \times 55\text{ mm}$) was used to produce homogeneous samples that were then cut into smaller pieces ($10 \times 10\text{ mm}$) for various experimental purposes.

SINTX Technologies Corporation, Salt Lake City, USA provided both the Si_3N_4 bulk samples and the Si_3N_4 powder used in this investigation. The bulk material, which was used as a positive control in biological testing, was prepared according to conventional ceramic fabrication techniques [19].

A Vision LWI VERGO-Workstation Nd:YAG laser with a wavelength of 1064 nm (max pulse energy: 70 joule, peak power 17 kW, voltage range 160–500 V, pulse time 1–20 ms, spot size 250–2000 μm) was used to clad the polyethylene with a silicon nitride powder coating.

The parameters used for laser coating were: voltage 225 V, pulse time 4 ms, and a spot size of 2000 μm . The laser coating apparatus was operated under a constant flux of nitrogen gas in order to prevent PE oxidation. The Si_3N_4 powder was spread on the PE surface and then treated with the laser beam to melt the material surface.

Silicon nitride powder (diameter between 5 μm and 25 μm) was deposited on the polyethylene surface and heated using the laser beam for it to be embedded into the polymeric matrix.

2.2. Samples Characterization

Raman spectra were collected at room temperature using a single monochromator (T-64000, Jobin-Ivon/Horiba Group, Kyoto, Japan) equipped with a 1024×256 pixels CCD camera (CCD-3500V, Horiba Ltd., Kyoto, Japan) and analyzed using commercially available software (LabSpec, Horiba/Jobin-Yvon, Kyoto, Japan). The excitation frequency used in all the experiments was the 532 nm green line of an Ar-ion laser operating at a nominal power of 280 mW.

The surface morphology was characterized using a confocal scanning laser microscope (Laser Microscope 3D and Profile measurements, Keyence, VKx200 Series, Osaka, Japan) capable of high-resolution optical images with depth selectivity. All images were collected at $50\times$ magnification. The roughness of each sample was measured and averaged over 25 random locations.

Scanning Electron Microscopy (SEM) and Energy Dispersive X-ray Spectroscopy (EDS) (JSM-7001F, JEOL, Tokyo, Japan) were used to acquire high magnification images and chemical composition maps of samples.

2.3. Biological Testing

Staphylococcus epidermidis (14990[®]ATCC[™]) cells were cultured in heart infusion (HI) broth (Nissui, Tokyo, Japan) at 37 °C for 18 h and titrated by colony forming assay using brain heart infusion (BHI) agar (Nissui). Aliquots of 1×10^7 bacteria were diluted in 10 μ L of phosphate-buffered saline (PBS) at physiological pH and ionic strength. The samples were preliminarily UV sterilized and introduced into wells. To each well, 1 mL of the bacteria culture was added and incubated at 37 °C under aerobic conditions for 12, 24, and 48 h.

SaOS-2 human osteosarcoma cells were first cultured and incubated in 4.5 g/L glucose DMEM (D-glucose, L-Glutamine, Phenol Red, and Sodium Pyruvate) supplemented with 10% fetal bovine serum. They were allowed to proliferate within Petri dishes for about 24 h at 37 °C. The final SaOS-2 concentration was 5×10^5 cell/mL. The cultured cells were then deposited on the top surface of the samples, which were previously sterilized by exposure to UV-C light for 30 min. In osteoconductivity tests, cell seeding took place in an osteogenic medium which consisted of DMEM supplemented with about 50 μ g/mL ascorbic acid, 10 mM β -glycerol phosphate, 100 mM hydrocortisone, and ~10% fetal bovine calf serum. The samples were incubated up to 14 days at 37 °C. The medium was changed twice a week during the incubation period. Subsequently, the cells were stained for fluorescence microscopy with green dye to identify osteocalcin (Monoclonal, Clone 5-12H, dilution 1:500, TakaraBio, Kusatsu-shi, Japan) and red dye to show the osteopontin (Osteopontin, O-17, Rabbit IgG, 1:500, IBL, Maebashi-Shi, Gunma, Japan).

3. Experimental Results

3.1. Surface Characterizations of Pristine and Coated Substrates

Laser microscopy images and their relative three-dimensional plots are shown in Figure 1. The surface of the bulk Si₃N₄ sample (Figure 1a) appeared quite smooth ($R_a = 0.011 \pm 0.001 \mu\text{m}$) due to polishing [19]. A higher surface roughness was found for the PE bulk sample (Figure 1b) as a consequence of its preparation process (i.e., in particular, the surface roughness of the silicon rubber mold), resulting in a $R_a = 0.297 \pm 0.022 \mu\text{m}$. The laser-cladded polyethylene (Figure 1c) showed the highest roughness ($R_a = 0.602 \pm 0.138 \mu\text{m}$) among the investigated samples due to the presence of the Si₃N₄ particles embedded in the PE surface and the irregular re-melting of the polymer.

SEM images of the surface at higher magnification are provided in Figure 2. The surface of the untreated polyethylene (Figure 2a) appeared relatively smooth at low magnification, but revealed a lamellar structure with an average thickness of $3.5 \pm 0.6 \mu\text{m}$ when observed under higher resolution. The morphology of the PE surface modified with Si₃N₄ cladding (Figure 2b) was characterized by the presence of Si₃N₄ particles partially embedded in the PE matrix. Micro-sized porosities can be observed on the surface due to the cleaning process: some silicon nitride particles, not completely embedded into the matrix, were removed from the treated surface during washing. The dimension of the particles was inhomogeneous (diameter between 5 and 25 μm) and the distribution of the Si₃N₄ particles was non-uniform across the surface.

A colored EDS map obtained at 1000 \times magnification (Figure 3) was used to check the distribution of carbon (green) as a marker for the presence of polyethylene matrix. As expected, the silicon signal (red) was concentrated at the ceramic particles with only limited overlap with the carbon signal in the regions where the particles were embedded in the matrix (cf. surface analysis on the left side of Figure 3). In a cross-section analysis (cf. on the right side of Figure 3), it was observed that the Si₃N₄ particles did not penetrate deeply into the PE matrix. It was also observed that most of the particles

were embedded to about 50%~70% of their external surface, leaving the remaining area exposed to the environment.

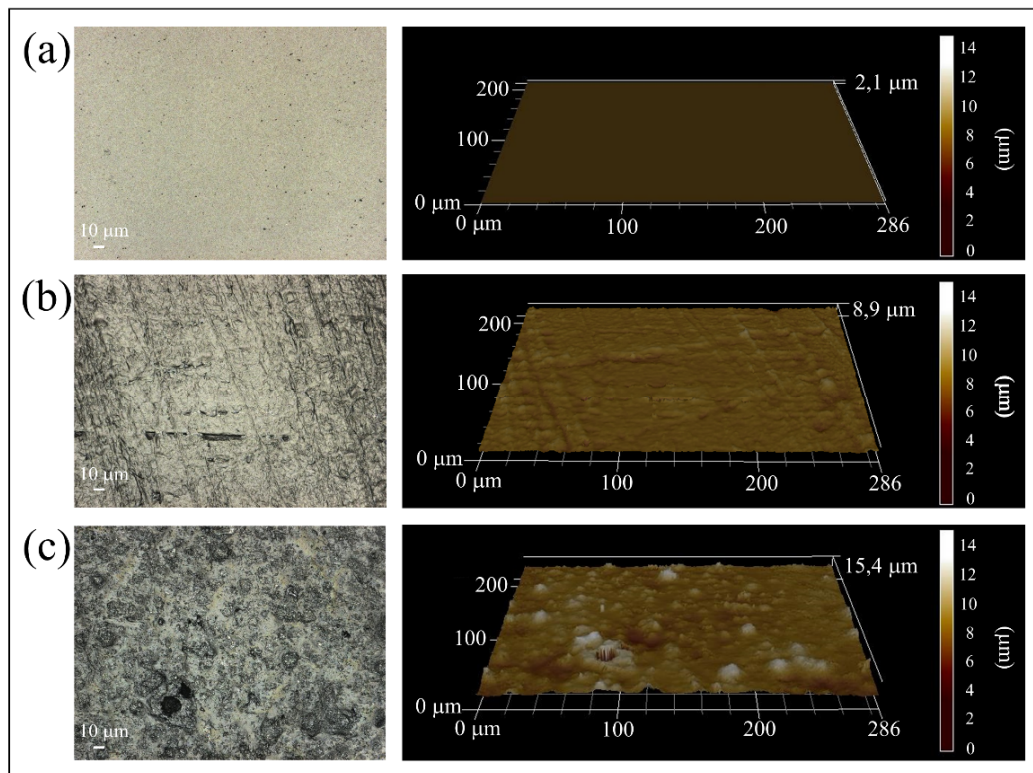


Figure 1. Laser microscopy images (left side) and relative topographic data (right side) of (a) bulk silicon nitride, (b) untreated polyethylene matrix and (c) polyethylene matrix combined with Si_3N_4 powders.

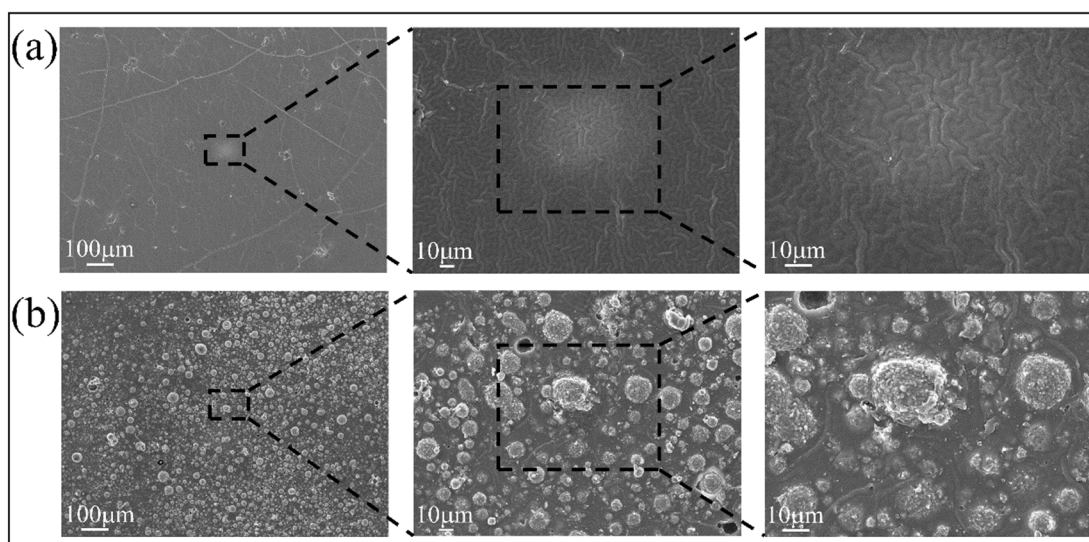


Figure 2. SEM images of (a) untreated polyethylene and (b) Si_3N_4 -coated PE substrate at different magnifications.

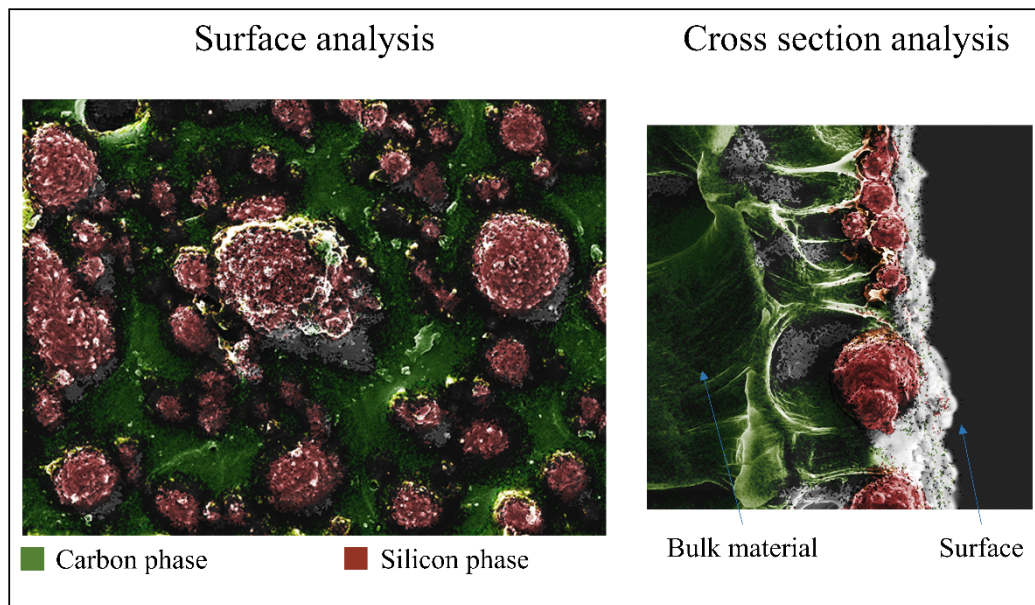


Figure 3. EDS maps of the Si_3N_4 -coated PE substrate; surface analysis and cross section analysis on the left and right side, respectively.

Incorporation of Si_3N_4 onto the PE surface was confirmed by Raman spectroscopy. Figure 4 shows the Raman spectra of the different samples: (a) bulk Si_3N_4 (reference material), (b) low density PE, and (c) laser-cladded PE. Table 1 shows the band assignment relative to both raw materials. The strong Si_3N_4 bands at about 200 cm^{-1} in (c) confirm the presence of the $\beta\text{-Si}_3\text{N}_4$ phase, but also other weaker vibrations, in particular, those related to the E_{2g} mode are still clearly visible [20].

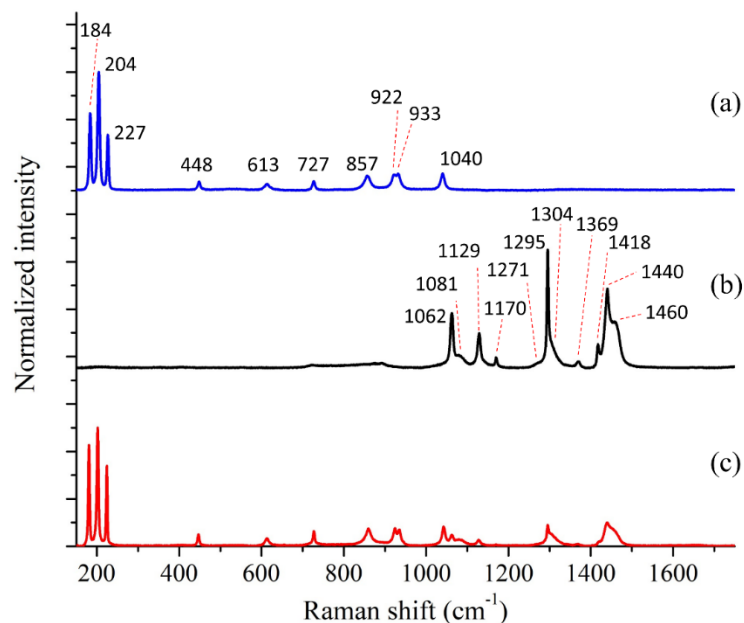


Figure 4. Raman spectra of 3 different samples: (a) bulk Si_3N_4 , (b) PE substrate, and (c) Si_3N_4 -coated PE substrate.

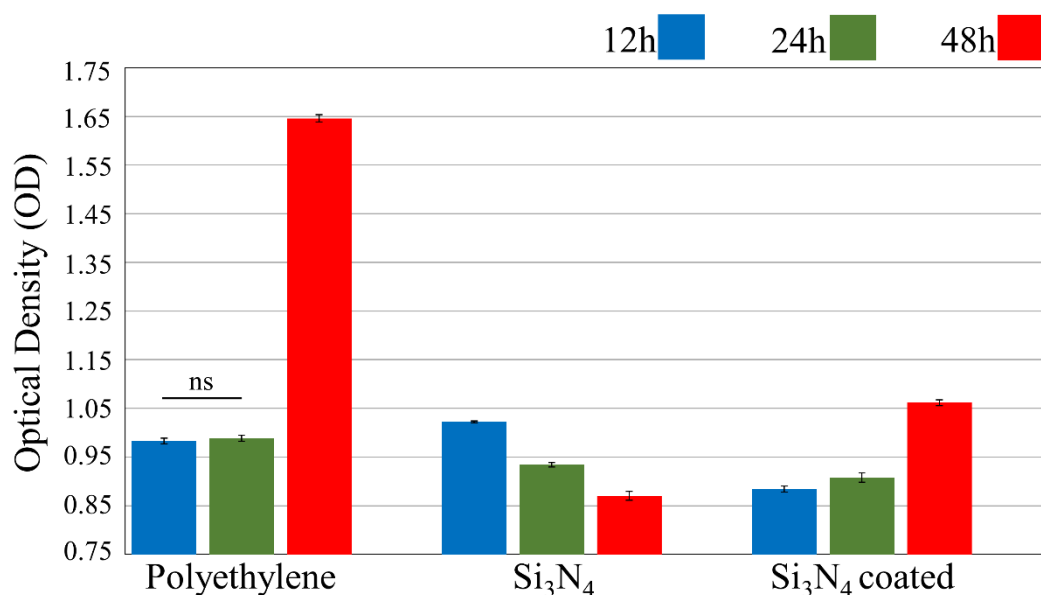
Table 1. Raman band assignments for Si₃N₄ (left) and PE (right).

Bands Position (cm ⁻¹)	Assignments	Bands Position (cm ⁻¹)	Assignments
184	E _{2g}	1062	C-C stretching
204	A _g	1081	C-C stretching
227	E _{1g}	1129	C-C stretching
448	E _{2g}	1170	CH ₂ rocking
613	E _{2g}	1271	CH ₂ twisting
727	A _g	1295	CH ₂ twisting
857	E _{1g}	1304	CH ₂ wagging
922	E _{2g}	1369	CH ₂ bending
933	A _g	1418	CH ₂ bending
1040	E _{2g}	1440	CH ₂ bending
		1460	CH ₂ rocking

Low density polyethylene Raman spectra (b) shows three main bands at 1062, 1081 and 1129 cm⁻¹ that represents the C-C stretching; additional bands (from 1170 to 1460 cm⁻¹) represent different bending modes of the CH₂ bonds [21]. In the Raman spectrum of cladded PE, polymer-related bands were weaker due to the presence of the ceramic layer on the surface.

3.2. In Vitro Bacterial Testing

A Microbial viability assay (WST) showed the amount of live bacteria on different sample surfaces (Figure 5). After 12 h of exposure, the Si₃N₄-cladded PE showed a lower amount of living bacteria as compared with both the negative (bulk PE) and the positive (Si₃N₄) control. After 24 h the number of bacteria on both the pristine and the laser-cladded PE samples increased, with the latter still showing better antibacterial performance. It should be noted that the positive Si₃N₄ control, which showed a relatively higher amount of bacteria at 12 h, performed better at 24 h. This is in line with previous results on Si₃N₄, where the “activation” of the surface antibacterial effects reflects the kinetics of released nitrogen species, in particular when the surfaces are polished [22]. At the end of the treatment (48 h) the presence of the bacteria on the Si₃N₄-cladded PE exhibits twice as high amounts of bacteria as compared to 24 h, but the values of Optical Density are still lower compared with the negative control.

**Figure 5.** Biological assay of *Staphylococcus epidermidis* as a function of bacterial exposure time.

Fluorescence microscopy analyses (Figures 6 and 7) showed the presence of dead and living bacteria on the different substrates. Three stains were used to identify the different bacterial states: CFDA green stain was used for live bacteria, PI red stain for dead bacteria, and DAPI blue stain for the nuclei of the bacteria. At all testing times, the PE substrate (Figure 6) showed higher amounts of live bacteria on its surface. The number of dead bacteria was very low as compared to the total number of bacteria present on the surface (expressed by the number of nuclei stained blue). A greater number of bacteria were present on the surface of the Si_3N_4 -cladded PE (Figure 7, *cf.* blue stain), but most of them were dead (*cf.* red stain).

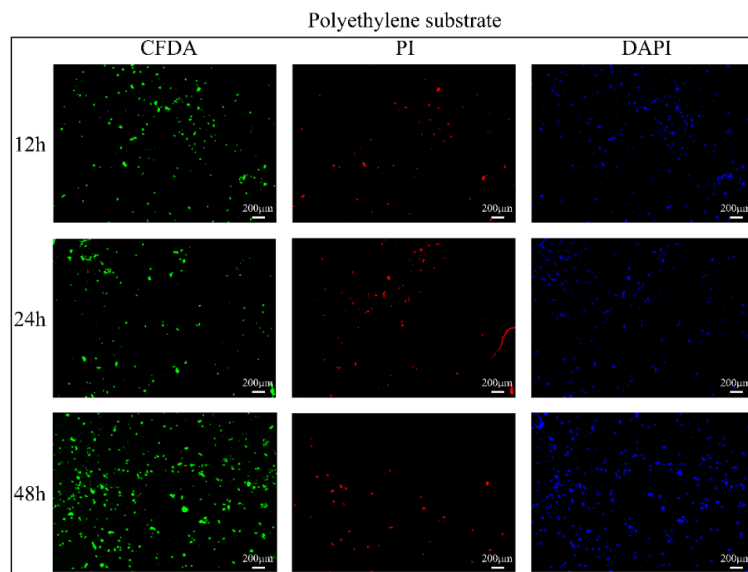


Figure 6. Fluorescence micrographs of the PE substrate after bacteria testing. Green stain (CFDA) marked the live bacteria, the red stain (PI) the dead bacteria, and the blue stain (DAPI) the bacterial cells' nuclei.

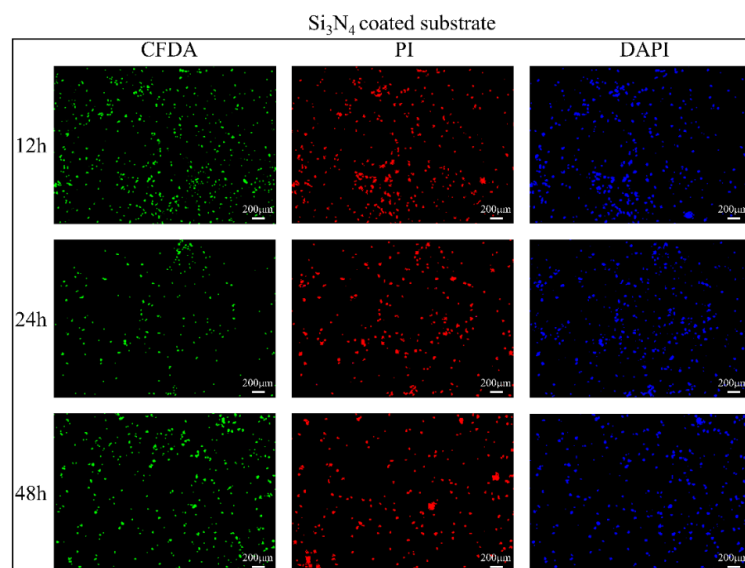


Figure 7. Fluorescence micrographs of the Si_3N_4 -coated PE substrate after bacteria testing. Green stain (CFDA) marked the live bacteria, the red stain (PI) the dead bacteria, and the blue stain (DAPI) the bacterial cells' nuclei.

3.3. In Vitro Osteosarcoma Testing

Figure 8 shows the laser micrographs of sample surfaces after SaOS-2 cells treatment. The positive control Si_3N_4 (Figure 8a) shows a large amount of bone tissue, consistent with previous observations [23]. Conversely, no bone tissue was formed on the bulk PE sample used as the negative control (Figure 8b). The Si_3N_4 -cladded PE surface (Figure 8c) showed an almost homogeneous distribution of hydroxyapatite particles (cf. white areas in the micrograph).

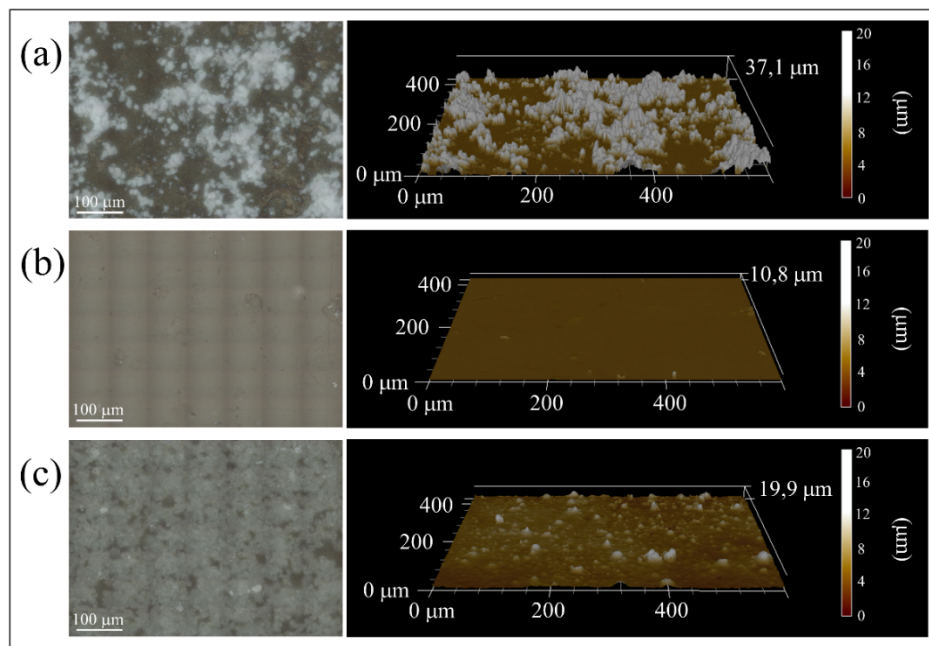


Figure 8. Laser microscopy images (left side) and relative topographic data (right side) of (a) bulk Si_3N_4 (positive control), (b) PE substrate, and (c) Si_3N_4 -coated PE substrate after SaOS-2 cell treatment.

The microbial viability assay (WST) results provide data on the number of living cells on the surface of the different samples (Figure 9). The Si_3N_4 -cladded PE surface showed lower cytotoxicity as compared to bulk PE and thus, higher cell proliferation. The data labeled as 2D represent cells in their medium without any substrate, as a positive control.

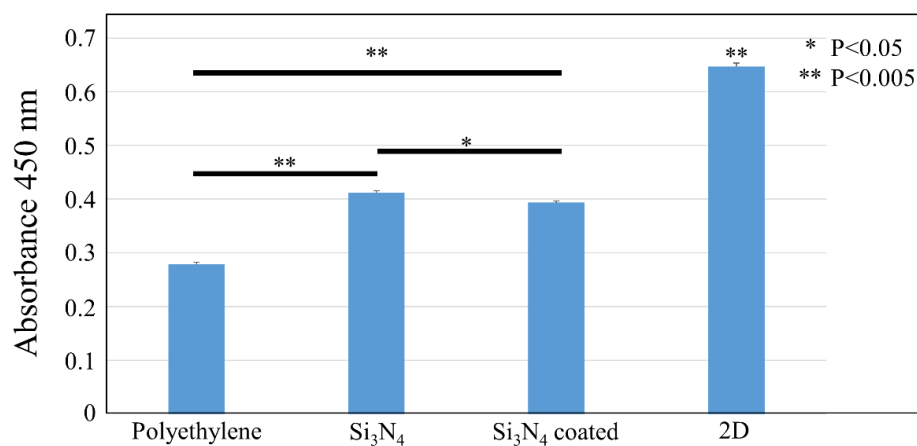


Figure 9. Biological assay (absorbance at 450 nm) of all the investigated samples after in vitro SaOS-2 cell exposure.

Fluorescence micrographs (Figure 10) indicate the presence of mineralized tissue by means of different stains: blue for cell nuclei; green for osteocalcin, and red for osteopontin. Both red and green markers suggest the presence of mineralized bone tissue. Bulk Si_3N_4 showed the highest amount of osteocalcin and osteopontin in the bone tissue synthesized by cells during the treatment, while the silicon nitride particles embedded in the PE surface increased the formation of hydroxyapatite crystal as compared to bulk PE.

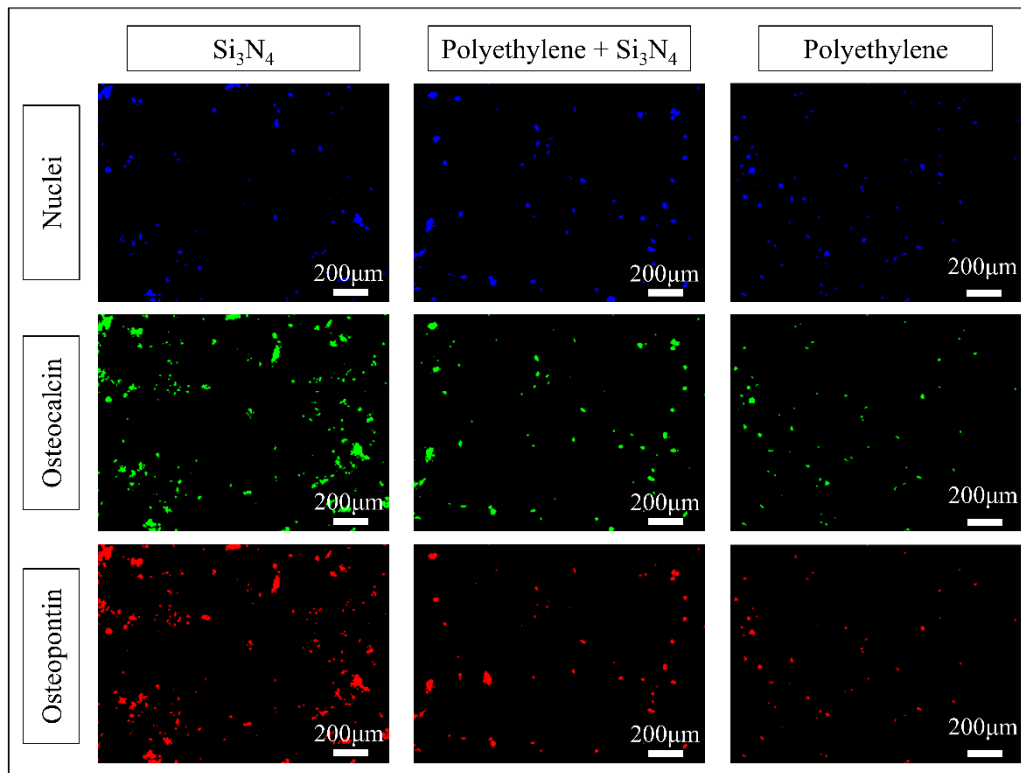


Figure 10. Fluorescence micrographs of the investigated samples after exposure to SaOS-2 cells. Green and red stain marked osteocalcin and osteopontin, respectively, while the blue stain located the cells' nuclei.

4. Discussion

Surface analyses showed that laser cladding could be suitable for producing a Si_3N_4 coating on the PE surface. Compared with prior studies using a Si_3N_4 coating on a Ti-alloy [24], the ceramic powders did not undergo chemical decomposition to form free Si. This might be due to the presence of a “soft” polymeric matrix that melted at relatively low power densities.

The presence of stoichiometric Si_3N_4 particles resulted in an active antibacterial effect. Previous work showed how Si_3N_4 in an aqueous environment generates ammonia that damages bacterial cells [25–27]. When compared to previous data, the antibacterial effect seems to act faster in the laser cladded coating, probably due to increased surface area.

Biological assays confirmed that the Si_3N_4 powders reduced the proliferation of bacteria on the PE coated surface as compared to bulk PE, especially after long-term exposure. Fluorescence microscopy analyses also confirmed the antibacterial effect of the Si_3N_4 coating. Additionally, the N and Si species released from Si_3N_4 enhanced cell proliferation and bone tissue formation [28–30].

In summary, the Si_3N_4 laser-cladded coating process was found to be capable of transferring the beneficial biological properties of bulk Si_3N_4 to PE.

5. Conclusions

In this work, polyethylene substrates were cladded with Si₃N₄ powder using a Nd:YAG laser. Biological testing showed that the silicon nitride coating provided both antibacterial and osteoconductive properties to the PE substrate. This new composite technology could be useful in improving antimicrobial and osteointegration characteristics of indwelling prosthetics made from polyethylene, as well as other applications that require less invasive contact with human biology.

Author Contributions: Data curation, M.Z. and F.B.; Formal analysis, M.Z., F.B. and T.A.; Methodology, T.Y., N.K. and B.S.B.; Supervision, E.M., W.Z., O.M. and G.P.; Visualization, R.A.; Writing—original draft, M.Z.; Writing—review & editing, E.M., B.J.M. and G.P. All authors have read and agreed to the published version of the manuscript.

Funding: This research received no external funding.

Conflicts of Interest: B.S.B. and B.J.M. are employees of SINTX Co. G.P. has been a consultant to SINTX Co. during the preparation of this work. The other authors declare no conflict of interest.

References

1. Teoh, S.H.; Tang, Z.G.; Hastings, G.W. Thermoplastic polymers in biomedical applications: Structures, properties and processing. In *Handbook of Biomaterial Properties*, 2nd ed.; Springer: Boston, MA, USA, 2016; pp. 261–290.
2. Fernández-Pradas, J.M.; Naranjo-León, S.; Morenza, J.L.; Serra, P. Surface modification of UHMWPE with infrared femtosecond laser. *Appl. Surf. Sci.* **2012**, *258*, 9256–9259. [[CrossRef](#)]
3. Riveiro, A.; Soto, R.; Comesaña, R.; Boutinguiza, M.; del Val, J.; Quintero, F.; Lusquiños, F.; Pou, J. Laser surface modification of PEEK. *Appl. Surf. Sci.* **2012**, *258*, 9437–9442. [[CrossRef](#)]
4. Lee, E.H.; Rao, G.R.; Lewis, M.B.; Mansur, L.K. Ion beam application for improved polymer surface properties. *Nucl. Inst. Methods Phys. Res. B* **1993**, *74*, 326–330. [[CrossRef](#)]
5. Chan, C.M.; Ko, T.M.; Hiraoka, H. Polymer surface modification by plasmas and photons. *Surf. Sci. Rep.* **1996**, *24*, 1–54. [[CrossRef](#)]
6. Riveiro, A.; Soto, R.; del Val, J.; Comesaña, R.; Boutinguiza, M.; Quintero, F.; Lusquiños, F.; Pou, J. Laser surface modification of ultra-high-molecular-weight polyethylene (UHMWPE) for biomedical applications. *Appl. Surf. Sci.* **2014**, *302*, 236–242. [[CrossRef](#)]
7. Ramakrishna, S.; Mayer, J.; Wintermantel, E.; Leong, K.W. Biomedical applications of polymer-composite materials: A review. *Compos. Sci. Technol.* **2001**, *61*, 1189–1224. [[CrossRef](#)]
8. Chan, C.M.; Cheng, C.L.; Yuen, M.M.F. Electrical properties of polymer composites prepared by sintering a mixture of carbon black and ultra-high molecular weight polyethylene powder. *Polym. Eng. Sci.* **1997**, *37*, 1127–1136. [[CrossRef](#)]
9. Thongruang, W.; Balik, C.M.; Spontak, R.J. Volume-exclusion effects in polyethylene blends filled with carbon black, graphite, or carbon fiber. *J. Polym. Sci. Part B Polym. Phys.* **2002**, *40*, 1013–1025. [[CrossRef](#)]
10. Hashimoto, M.; Takadama, H.; Mizuno, M.; Yasutomi, Y.; Kokubo, T. Titanium dioxide/ultra high molecular weight polyethylene composite for bone-repairing applications: Preparation and biocompatibility. *Key Eng. Mater.* **2003**, *240–242*, 415–418. [[CrossRef](#)]
11. Roy, S.; Pal, S. Characterization of silane coated hollow sphere alumina-reinforced ultra high molecular weight polyethylene composite as a possible bone substitute material. *Bull. Mater. Sci.* **2002**, *25*, 609–612. [[CrossRef](#)]
12. Suwanprateeb, J. Binary and ternary particulated composites: UHMWPE/CaCO₃/HDPE. *J. Appl. Polym. Sci.* **2000**, *75*, 1503–1513. [[CrossRef](#)]
13. Fang, L.; Leng, Y.; Gao, P. Processing of hydroxyapatite reinforced ultrahigh molecular weight polyethylene for biomedical applications. *Biomaterials* **2005**, *26*, 3471–3478. [[CrossRef](#)] [[PubMed](#)]
14. Anderson, B.C.; Bloom, P.D.; Baikerikar, K.G.; Sheares, V.V.; Mallapragada, S.K. Al-Cu-Fe quasicrystal/ultra-high molecular weight polyethylene composites as biomaterials for acetabular cup prosthetics. *Biomaterials* **2002**, *23*, 1761–1768. [[CrossRef](#)]
15. Bal, B.S.; Rahaman, M.N. Orthopedic Applications of Silicon Nitride Ceramics. *Acta Biomater.* **2012**, *8*, 2889–2898. [[CrossRef](#)] [[PubMed](#)]

16. Bock, R.M.; Jones, E.N.; Ray, D.A.; Sonny Bal, B.; Pezzotti, G.; McEntire, B.J. Bacteriostatic behavior of surface modulated silicon nitride in comparison to polyetheretherketone and titanium. *J. Biomed. Mater. Res. Part A* **2017**, *105*, 1521–1534. [[CrossRef](#)] [[PubMed](#)]
17. Webster, T.J.; Patel, A.A.; Rahaman, M.N.; Sonny Bal, B. Anti-infective and osteointegration properties of silicon nitride, poly(ether ether ketone), and titanium implants. *Acta Biomater.* **2012**, *8*, 4447–4454. [[CrossRef](#)]
18. Pezzotti, G.; Marin, E.; Adachi, T.; Lerussi, F.; Rondinella, A.; Boschetto, F.; Zhu, W.; Kitajima, T.; Inada, K.; McEntire, B.J.; et al. Incorporating Si₃N₄ into PEEK to Produce Antibacterial, Osteoconductive, and Radiolucent Spinal Implants. *Macromol. Biosci.* **2018**, *18*, e1800033. [[CrossRef](#)]
19. McEntire, B.J.; Lakshminarayanan, R.; Thirugnanasambandam, P.; Seitz-Sampson, J.; Bock, R.; O'Brien, D. Processing and Characterization of Silicon Nitride Bioceramics. *Bioceram. Dev. Appl.* **2016**, *6*, 1000093. [[CrossRef](#)]
20. Honda, K.; Yokoyama, S.; Tanaka, S. Assignment of the Raman Active Vibration Modes of β -Si₃N₄ using Micro-Raman Scattering. *J. Appl. Phys.* **1999**, *85*, 7380–7384. [[CrossRef](#)]
21. Sato, H.; Shimoyama, M.; Kamiya, T.; Amari, T.; Šašić, S.; Ninomiya, T.; Siesler, H.W.; Ozaki, Y. Raman spectra of high-density, low-density, and linear low-density polyethylene pellets and prediction of their physical properties by multivariate data analysis. *J. Appl. Polym. Sci.* **2002**, *86*, 443–448. [[CrossRef](#)]
22. Yoda, I.; Koseki, H.; Tomita, M.; Shida, T.; Horiuchi, H.; Sakoda, H.; Osaki, M. Effect of Surface Roughness of Biomaterials on Staphylococcus Epidermidis Adhesion. *BMC Microbiol.* **2014**, *14*, 234. [[CrossRef](#)]
23. Pezzotti, G.; Bock, R.M.; Adachi, T.; Rondinella, A.; Boschetto, F.; Zhu, W.; Marin, E.; McEntire, B.J.; Sonny Bal, B.; Mazda, O. Silicon Nitride Surface Chemistry: A Potent Regulator of Mesenchymal Progenitor Cell Activity in Bone Formation. *Appl. Mater. Today* **2017**, *9*, 82–95. [[CrossRef](#)]
24. Zanicco, M.; Boschetto, F.; Zhu, W.; Marin, E.; McEntire, B.J.; Sonny Bal, B.; Adachi, T.; Yamamoto, T.; Kanamura, N.; Ohgitani, E.; et al. 3D-Additive Deposition of an Antibacterial and Osteogenic Silicon Nitride Coating on Orthopaedic Titanium Substrate. *J. Mech. Behav. Biomed. Mater.* **2020**, *103*, 103557. [[CrossRef](#)] [[PubMed](#)]
25. Pezzotti, G.; Bock, R.M.; McEntire, B.J.; Adachi, T.; Marin, E.; Boschetto, F.; Zhu, W.; Mazda, O.; Sonny Bal, B. In vitro Antibacterial Activity of Oxide and Non-Oxide Bioceramics for Arthroplastic Devices: I. In situ Time-Lapse Raman Spectroscopy. *Analyst* **2018**, *143*, 3708–3721. [[CrossRef](#)] [[PubMed](#)]
26. Himathongkham, S.; Riemann, H. Destruction of Salmonella typhimurium, Escherichia coli O157:H7 and Listeria monocytogenes in Chicken Manure by Drying and/or Gassing with Ammonia. *FEMS Microbiol. Lett.* **1999**, *171*, 179–182. [[CrossRef](#)] [[PubMed](#)]
27. Kim, Y.M.; Farrah, S.; Baney, R.H. Membrane Damage of Bacteria by Silanols Treatment. *Electron. J. Biotechnol.* **2007**, *10*, 252–259. [[CrossRef](#)]
28. Marin, E.; Rondinella, A.; Boschetto, F.; Zanicco, M.; McEntire, B.J.; Sonny Bal, B.; Pezzotti, G. Understanding Silicon Nitride's Biological Properties: From Inert to Bioactive Ceramic. *Key Eng. Mater.* **2018**, *782*, 289–296. [[CrossRef](#)]
29. Pezzotti, G.; Marin, E.; Adachi, T.; Rondinella, A.; Boschetto, F.; Zhu, W.; Sugano, N.; Bock, R.M.; McEntire, B.J.; Sonny Bal, B. Bioactive Silicon Nitride: A New Therapeutic Material for Osteoarthropathy. *Sci. Rep.* **2017**, *7*, 44848. [[CrossRef](#)]
30. Pezzotti, G.; McEntire, B.J.; Bock, R.M.; Boffelli, M.; Zhu, W.; Vitale, E.; Puppulin, L.; Adachi, T.; Yamamoto, T.; Kanamura, N.; et al. Silicon Nitride: A Synthetic Mineral for Vertebrate Biology. *Sci. Rep.* **2016**, *6*, 31717. [[CrossRef](#)]

